
IFSCC 2025 full paper (IFSCC2025-217)

How can the dynamics of polymers at the surface of cosmetic pigments be probed using solid-state NMR spectroscopy?

Nadine Melhem^{1,2}, Reiichiro Tsuchiya³, Andrew Rankin⁴, Olivier Lafon¹, Takehiro Goto³, Takumi Tanaka³, Tetsuya Takahashi²

¹ Univ. Lille, CNRS UMR 8181, UCCS, Lille, France; ² Miyoshi Europe SAS., Saint Priest, France; ³ Daito Kasei Kogyo Co., Ltd., Osaka, Japan; ⁴ Univ. Lille, CNRS FR 2638, IMEC, Lille, France.

1. Introduction

In 2017, the European Commission asked the European Chemicals Agency (ECHA) to evaluate scientific evidence for EU-level regulatory action on microplastics intentionally added to products as a precautionary measure against environmental hazard concerns. In response, ECHA presented a Q & A on July 10, 2019 as a proposal for the definition of microplastics in general [1]. Furthermore, on August 22, 2019, the detailed definition of microplastics was added to REACH [2]. At the same time, at the request of ECHA, the Risk Assessment Committee (RAC) and the Socio-Economic Analysis Committee (SEAC) submitted a written opinion on June 11, 2020 [3]. Some of the cosmetic pigments on the market today are surface-treated with polymers to improve "feel" and water resistance. According to the definition of microplastics added to REACH, all solid pigments containing polymers will be defined as microplastics and will be banned from manufacture and sale in 2026. There are two exclusions in this current provision: "Polymer content is 1% w/w or less and does not cover the entire surface of the pigment" or "Polymer is not solid". The surface treatment of cosmetic pigments with siloxane polymer does not cover the entire surface of the pigment, but it requires use of 1% or more to guarantee its functional effect. In this context, we have investigated the mobility of surface treatment agents, including polydimethylsiloxane (PDMS) and

polymethylhydrosiloxane (PMHS), also known as dimethicone and methicone, respectively, using ^1H , ^{13}C and ^{29}Si solid-state NMR spectroscopy, and how this data can be linked to the solid or liquid state of the polymers.

2. Materials and Methods

For this study, TiO_2 pigment was treated with three distinct surface pigment agents: low viscosity PDMS ($50 \text{ mm}^2/\text{s}$, i.e. liquid, denoted 50CS PDMS hereafter), high viscosity PDMS ($1,000,000 \text{ mm}^2/\text{s}$, i.e. liquid, but close to solid, denoted 1,000,000CS PDMS hereafter) and PHMS. For the three samples, the fraction of treatment agent was 2wt% of the whole amount of pigment.

One-dimensional (1D) ^1H , ^{13}C and ^{29}Si direct excitation as well as $^1\text{H} \rightarrow ^{13}\text{C}$ and $^1\text{H} \rightarrow ^{29}\text{Si}$ cross-polarization under magic-angle spinning (CPMAS) [4] and $^1\text{H} \rightarrow ^{13}\text{C}$ and $^1\text{H} \rightarrow ^{29}\text{Si}$ J-RINEPT [5] NMR spectra were recorded at $B_0 = 9.4 \text{ T}$, i.e. Larmor frequencies of 400 MHz for ^1H , 100 MHz for ^{13}C and 79 MHz for ^{29}Si , and 37 °C on a wide-bore magnet equipped with Bruker AVANCE III NMR console and Bruker double-resonance $^1\text{H}/\text{X}$ 4 mm or 7 mm magic-angle spinning (MAS) probes. The 4 mm probe was used for the ^1H and ^{13}C NMR experiments on PDMS/ TiO_2 samples, while the 7 mm probe was used for the ^{29}Si NMR experiments on PDMS/ TiO_2 samples as well as ^1H , ^{13}C and ^{29}Si NMR experiments on the PDMS/ TiO_2 samples. Powdered samples were packed into 4 or 7 mm outer diameter zirconia rotors with Kel-F drive caps and spun at a MAS rate, $v_R = 12.5$ or 5 kHz, respectively. ^1H and ^{13}C isotropic chemical shifts were referenced with respect to a solution of 1% tetramethylsilane (TMS) in CDCl_3 using the CH_2 group resonance of a solid sample of adamantane at 1.735 ppm (^1H) or 37.77 ppm (^{13}C) as a secondary reference. ^{29}Si isotropic chemical shift were referenced with respect to a solution of 1% tetramethylsilane (TMS) in CDCl_3 using the resonance of OSi(OMe)_3 group of octakis(trimethylsiloxy)silsesquioxane (Q_8M_8) at 11.35 ppm as a secondary reference. Temperature control was maintained using a Bruker “BCU-Xtreme” variable temperature unit. The temperature value at the sample was determined by observation of the ^{207}Pb chemical shift of a solid sample of $\text{Pb}(\text{NO}_3)_2$ as a function of thermocouple readout [6].

Proton NMR spectra were acquired by averaging 16 transients, separated by a recycle interval of 5 s, using the DEPTH pulse sequence for probe background suppression [7]. For protons, the longitudinal relaxation time, T_1 (^1H), and the time constant associated with the homogeneous contribution to dephasing, T_2' (^1H), were measured using saturation-recovery and Hahn echo sequences, respectively.

All ^{13}C NMR spectra were acquired using SW_r-TPPM ^1H decoupling [8] during the acquisition for 4 and 7 mm probes. ^{13}C direct excitation NMR spectra were acquired by averaging between 1024 and 6400 transients, depending on the sample, separated by a recycle interval of 60 s, using the DEPTH pulse sequence for probe background suppression [7]. A $\pi/4$ pulse was used for the first pulse. $^1\text{H} \rightarrow ^{13}\text{C}$ CPMAS NMR experiments were acquired with CP contact times $\tau_{\text{CP}} = 2.5$ or 25 ms. $^1\text{H} \rightarrow ^{13}\text{C}$ CPMAS spectra were recorded using recycle intervals equal to $1.3T_1$ (^1H) to maximize the sensitivity [9], and were the result of averaging between 4096 and 16384 transients, depending on the sample. $^1\text{H} \rightarrow ^{13}\text{C}$ J-RINEPT experiments were acquired with defocusing and refocusing delays of $\tau_1 = 2.08$ ms and $\tau_2 = 0.69$ ms using recycle intervals equal to $1.3T_1$ (^1H). The $^1\text{H} \rightarrow ^{13}\text{C}$ J-RINEPT spectra were the result of averaging 4096 transients.

All ^{29}Si NMR spectra were acquired using SW_r-TPPM ^1H decoupling [8]. The 1D ^{29}Si direct excitation NMR spectra were acquired by averaging either 512 or 2048 transients separated by a recycle interval of 60 s. A $\pi/6$ pulse was used for the first pulse. The $^1\text{H} \rightarrow ^{29}\text{Si}$ CP MAS NMR experiments were acquired with CP contact time $\tau_{\text{CP}} = 2.5$ or 25 ms. Spectra resulted from averaging 4096 and 16384 transients depending on the sample separated by recycle intervals equal to $1.3T_1$ (^1H) to maximize the sensitivity [8]. $^1\text{H} \rightarrow ^{29}\text{Si}$ J-RINEPT NMR experiments were acquired with defocusing and refocusing delays of $\tau_1 = 35.7$ ms and $\tau_2 = 11.9$ ms. $^1\text{H} \rightarrow ^{29}\text{Si}$ J-RINEPT spectra resulted from averaging 4096 transients separated by recycle interval of $1.3T_1$ (^1H). Data processing and analysis was performed using Bruker TopSpin, ssNake [10] and Gnuplot.

3. Results

^1H solid-state NMR

The 1D ^1H MAS NMR spectra of TiO_2 particles treated with 50CS PDMS and 1,000,000CS PDMS are shown in Figure 1. These spectra exhibit narrow signals at -0.1 ppm assigned to the CH_3 groups of PDMS chains. The ^1H resonances of these two samples exhibit similar linewidth. This observation indicates CH_3 of PDMS chains show fast motions in both low and high viscosity PDMS. This result is consistent with the similar $T_2'(^1\text{H})$ values, which are equal to 11.8 and 11.4 ms for CH_3 groups of 50CS and 1,000,000CS PDMS chains, respectively.

The 1D ^1H spectrum PMHS-treated TiO_2 , displayed in Figure 2, exhibits two main ^1H signals: an intense peak resonating at 0.11 ppm assigned to the methyl group of PMHS chains as well as a weaker signal at 4.7 ppm assigned to SiH protons [11]. This quantitative spectrum was simulated using the ssNake software [10] and shows that the integrated intensity of CH_3 signals is 3.6 times larger than that of SiH signals for TiO_2 particles functionalized with PMHS, instead of 3 for the pristine PMHS polymer. This result indicates that one sixth of SiH groups of PMHS reacts with surface hydroxyl groups of TiO_2 particles to form $\text{Si}-\text{O}-\text{Ti}$ covalent bonds. In addition, the measured $T_2'(^1\text{H})$ relaxation times indicate that PMHS sample contains both mobile polymer chains with long T_2' (24 ms), and rigid chains with a short T_2' (1 ms). The fractions of rigid and mobile polymer chains are approximately equal.

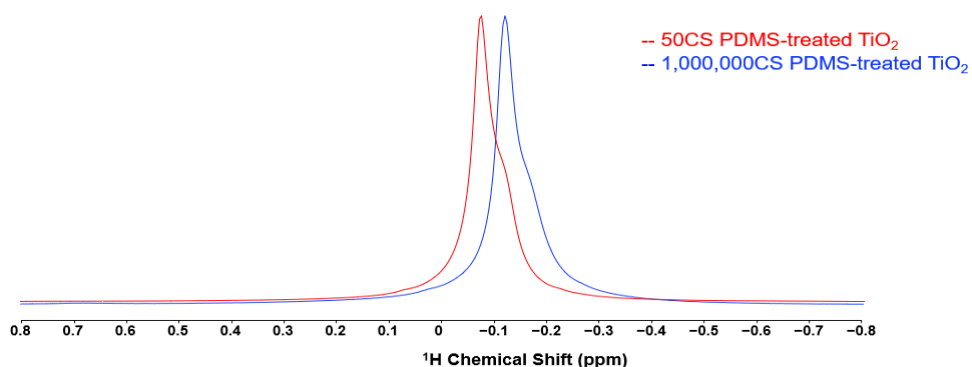


Figure 1. 1D ^1H MAS NMR spectra of TiO_2 particles treated with 50CS PDMS (red), 1,000,000CS PDMS (blue) at $B_0 = 9.4$ T with $v_R = 12.5$ kHz.

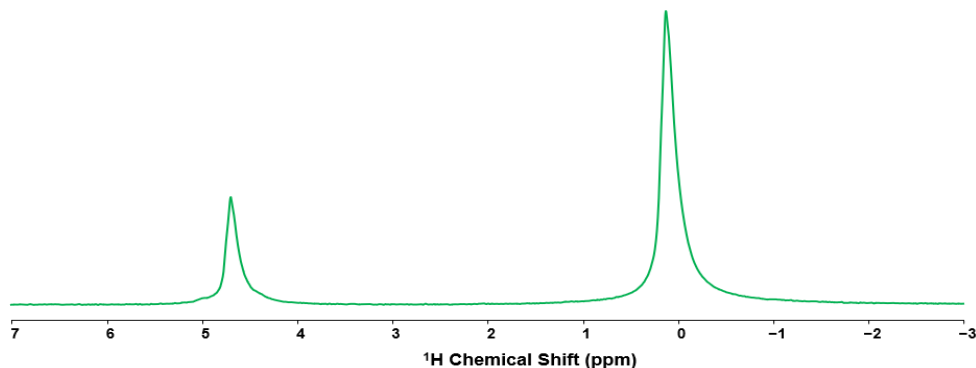


Figure 2. 1D ¹H MAS NMR spectra of TiO₂ particles with PMHS acquired at $B_0 = 9.4$ T with $v_R = 5$ kHz.

¹³C solid-state NMR

The mobility of polymer chains on the surface of TiO₂ particles was also probed by recording and comparing 1D ¹³C NMR spectra acquired with ¹H→¹³C CPMAS and J-RINEPT polarization transfers as well as direct excitation sequence. A signal in CPMAS spectrum can be observed for rigid molecular segments with slow and/or anisotropic motions since the ¹H→¹³C CP transfer is mediated by ¹H-¹³C dipolar couplings, which are averaged out by fast isotropic reorientation. Conversely, the ¹H→¹³C J-RINEPT experiment allows for the observation of mobile segments since the ¹H transverse magnetization rapidly decays under ¹H-¹H dipolar couplings during the defocusing delay of J-RINEPT experiment. Segments with rapid but anisotropic motions produce signals in both CPMAS and J-RINEPT spectra. The ¹³C direct-excitation NMR experiment allows the observation of all molecular segments. Figures 3a and b compare the ¹H→¹³C CPMAS and J-RINEPT NMR spectra as well as the ¹³C direct excitation NMR spectrum of 50CS and 1,000,000CS PDMS-treated TiO₂, respectively. Both samples exhibit similar lineshapes for the four spectra. These results indicate that these two samples contain both mobile and rigid PDMS chains. Nevertheless, from these spectra, it is not possible to estimate the fractions of mobile and rigid chains since the linewidths of CPMAS and J-RINEPT NMR spectra are comparable. As seen in Figure 3c, signals are also detected in the ¹H→¹³C CPMAS, J-RINEPT and ¹³C direct-excitation NMR spectra of PMHS-treated TiO₂ particles. This result indicates that this sample contains both rigid and mobile PMHS polymer.

Nevertheless, the ^{13}C direct excitation signal of this sample is significantly broader than that of $^1\text{H} \rightarrow ^{13}\text{C}$ J-RINEPT spectrum and has a width similar to that of the $^1\text{H} \rightarrow ^{13}\text{C}$ CPMAS spectrum acquired with $\tau_{\text{CP}} = 25$ ms. The $^1\text{H} \rightarrow ^{13}\text{C}$ CPMAS spectrum acquired with $\tau_{\text{CP}} = 2.5$ ms is broader than that obtained using $\tau_{\text{CP}} = 25$ ms and ^{13}C direct excitation. These results indicates that the fraction of rigid PMHS chains is significant, in agreement with measured $T_2'(^1\text{H})$ values. The peaks observed from CPMAS and direct excitation experiments on sample PMHS-treated TiO_2 are noticeably broader than those of PDMS-treated TiO_2 samples analyzed. This broadening suggests that polymer chains are more rigid in PMHS/ TiO_2 than in PDMS/ TiO_2 samples.

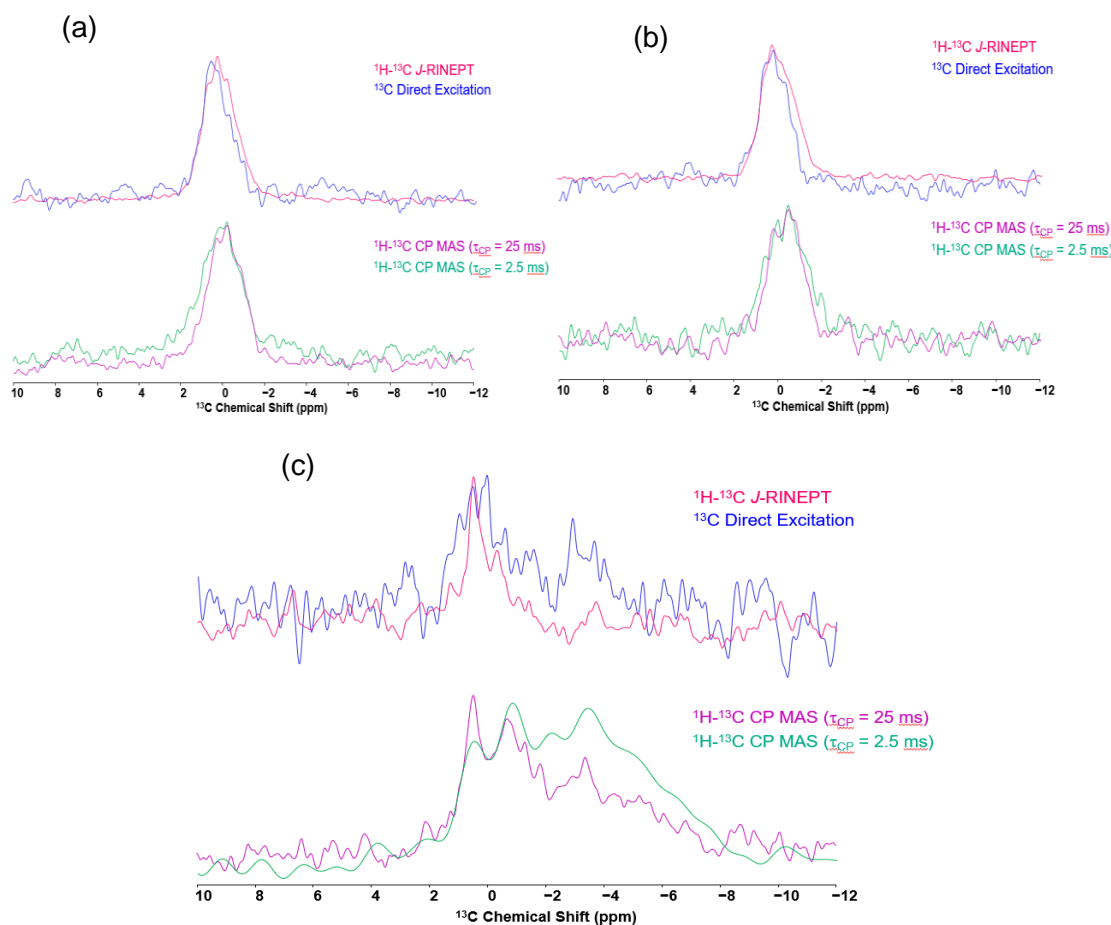


Figure 3. 1D ^{13}C MAS NMR spectra of TiO_2 particles treated with (a) 50CS PDMS, (b) 1,000,000CS PDMS and (c) PMHS acquired using $^1\text{H} \rightarrow ^{13}\text{C}$ CPMAS with $\tau_{\text{CP}} = 2.5$ (green) or 25 ms (purple), or J-RINEPT (red) polarization transfers, or direct excitation (blue) at $B_0 = 9.4$ T with $\nu_R = 12.5$ kHz for

PDMS/TiO₂ samples and 5 kHz for PHMS/TiO₂ sample. In the three panels, the spectra are normalized to the same maximal intensity.

²⁹Si solid-state NMR

The mobility of polymer chains on the surface of TiO₂ particles was also probed by recording and comparing 1D ²⁹Si NMR spectra acquired with ¹H → ²⁹Si CPMAS and *J*-RINEPT polarization transfers as well as direct excitation. Figure 4 displays the comparison of ²⁹Si spectra of both PDMS/TiO₂ samples. These spectra only exhibit a signal near -23 ppm assigned to D² site (Si(OSi)₂(CH₃)₂). No signal from T sites (SiO₃CH₃) between -40 and -70 ppm is detected. In 50CS PDMS/TiO₂, the ²⁹Si direct excitation and ¹H → ²⁹Si *J*-RINEPT spectra exhibit similar lineshapes. This result indicates that most polymer chains in this sample are mobile. Nevertheless, ¹H → ²⁹Si CPMAS spectra exhibit some signals. Hence, a small fraction of PDMS polymer chains are rigid. These rigid polymer chains may be located near the surface. In contrast, the ²⁹Si direct-excitation spectrum of 1,000,000CS PDMS/TiO₂ exhibits both broad and narrow components, indicating a mixture of rigid and mobile chains. This larger fraction of rigid polymer may stem from the presence of entanglements. Furthermore, ¹H → ²⁹Si *J*-RINEPT and CPMAS spectra (with $\tau_{CP} = 25$ ms) are broader for 1,000,000CS PDMS than for 50CS PDMS. The results are consistent with higher viscosity of 1,000,000CS PDMS.

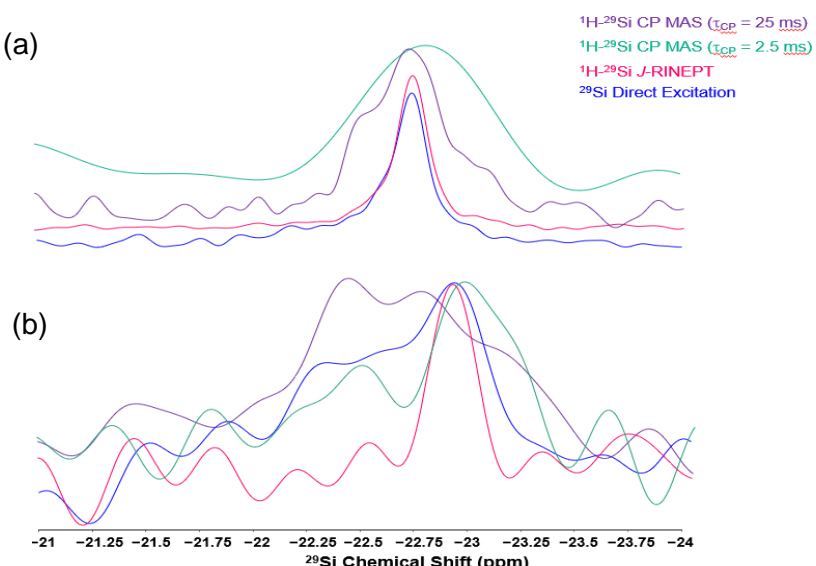


Figure 4. 1D ²⁹Si MAS NMR spectra of TiO₂ particles treated with (a) 50CS PMDS and (b) 1,000,000CS PDMS acquired using ¹H → ²⁹Si CPMAS with $\tau_{CP} = 2.5$ (green) or 25 ms (purple), or *J*-RINEPT (red) polarization transfers, or direct excitation (blue) at $B_0 = 9.4$ T with $v_R = 5$ kHz. The spectra are normalized to the same maximal intensity.

Figure 5 shows a comparison of ^{29}Si NMR spectra of PMHS/TiO₂ acquired with $^1\text{H} \rightarrow ^{29}\text{Si}$ CPMAS and *J*-RINEPT polarization transfers as well as direct excitation. The ^{29}Si direct excitation and $^1\text{H} \rightarrow ^{29}\text{Si}$ CPMAS spectra exhibit signals at -35.5, -58 and -67 ppm assigned to D² ($\text{Si(OSi)}_2(\text{H})\text{CH}_3$), T² (including $\text{Si(OSi)}_2(\text{OH})\text{CH}_3$ and $\text{Si(OSi)}_2(\text{OTi})\text{CH}_3$ species since OH and OTi groups have similar influence on isotropic chemical shift of bonded ^{29}Si nucleus [12],[13]) and T³ ($\text{Si(OSi)}_3\text{CH}_3$), respectively. $\text{Si(OSi)}_2(\text{OTi})\text{CH}_3$ species correspond to surface sites formed by the reaction of SiH sites with OH groups on the surface of TiO₂ pigment, whereas $\text{Si(OSi)}_3\text{CH}_3$ corresponds to cross-links between polymer chains formed by the reaction between two SiH groups and water. The signals of T sites are not detected in the *J*-RINEPT spectrum, which shows their rigidity. Furthermore, D² signals observed in direct-excitation and CPMAS spectra exhibit similar linewidth, whereas narrower resonance is detected for these sites in the *J*-RINEPT spectrum. This result indicates that the majority of D² sites in PMHS/TiO₂ sample is rigid. Nevertheless, the presence of D² signal in the *J*-RINEPT spectrum shows that a small fraction of D² sites are mobile in PMHS chains.

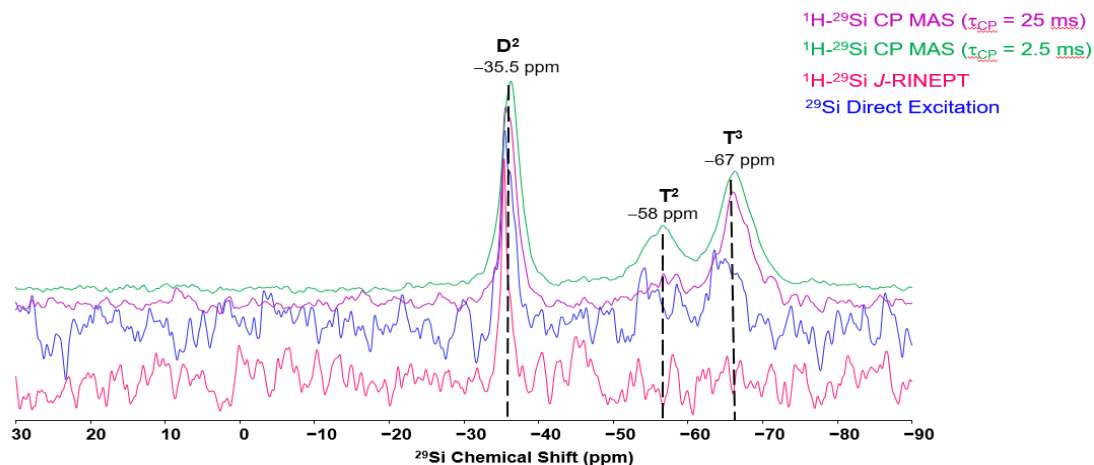


Figure 5. 1D ^{29}Si MAS NMR spectra of TiO₂ particles treated with PMHS acquired using $^1\text{H} \rightarrow ^{29}\text{Si}$ CPMAS with $\tau_{\text{CP}} = 2.5$ (green) or 25 ms (purple), or *J*-RINEPT (red) polarization transfers, or direct excitation (blue) at $B_0 = 9.4$ T with $v_R = 5$ kHz. The spectra are normalized to the same maximal intensity.

4. Discussion

The above ^1H , ^{13}C and ^{29}Si NMR data indicate difference in mobility between the polymers 50CS PDMS, 1,000,000CS PDMS and PMHS when they are used for the surface treatment of TiO₂ particles. In the case of 50CS PDMS, most polymer chains are highly mobile, even if a

small fraction of polymer near the surface is rigid. These rigid segments probably correspond to polymer chains close to the TiO₂ surface [14,15,16]. In contrast, 1,000,000CS PDMS contains a mixture of mobile and rigid chains in similar proportions. The larger fraction of rigid chains for that sample is consistent with the higher viscosity of the polymer and probably stems from the presence of entanglements. For PMHS, approximately one-sixth of the SiH groups react with hydroxyl groups of TiO₂ surface, forming Si–O–Ti links. These links restrict the mobility of PMHS chains and hence, most polymer chains in this sample are rigid, even if a small amount of mobile D² sites is detected.

5. Conclusion

The molecular mobility of PHMS-treated TiO₂ and PDMS-treated TiO₂ were evaluated by ¹H, ¹³C and ²⁹Si NMR measurements. The obtained NMR results indicate that 50CS PDMS/TiO₂ contains a majority of mobile polymer chains, even if a small fraction of rigid chains are detected near the surface of TiO₂ particles. In 1,000,000CS PDMS/TiO₂ sample, rigid and mobile chains are detected in similar proportions. The higher fraction of rigid chains is consistent with the higher viscosity and the formation of entanglements. Finally, PMHS/TiO₂ contains a majority of rigid polymer chains, even if a small amount of mobile segments is detected. This higher rigidity stems from the formation of Si–O–Ti links between the PMHS chains and the TiO₂ surface as well as Si–O–Si cross-links between polymer chains since about one-sixth of the SiH groups is consumed during the pigment surface treatment with PMHS.

References

- [1] Helsinki, Restriction proposal on intentionally-added microplastics – questions and answers, European Chemicals Agency (ECHA), 2020.
- [2] Annex to Annex XV Restriction Report, substance name: Intentionally Added Microplastics, version 1.2, European Chemicals Agency (ECHA), 2019.
- [3] Opinion on an Annex XV dossier proposing restrictions on intentionally-added microplastics, Committee for Risk Assessment (RAC) Committee for Socio-economic Analysis (SEAC), 2020.

- [4] A. Pines *et al.*, Proton-Enhanced Nuclear Induction Spectroscopy. A Method for High Resolution NMR of Dilute Spins in Solids, *J. Chem. Phys.*, 56, 1776–1777, 1972.
- [5] G. A. Morris *et al.*, Enhancement of nuclear magnetic resonance signals by polarization transfer, *J. Am. Chem. Soc.*, 101, 760–762, 1979.
- [6] A. Bielecki *et al.*, Temperature Dependence of ^{207}Pb MAS Spectra of Solid Lead Nitrate. An Accurate, Sensitive Thermometer for Variable-Temperature MAS, *J. Magn. Reson. A*, 116, 215–220, 1995.
- [7] D. G. Cory *et al.*, Suppression of signals from the probe in bloch decay spectra, *J. Magn. Reson.*, 80, 128–132, 1988.
- [8] R. S. Thakur *et al.*, Swept-frequency two-pulse phase modulation for heteronuclear dipolar decoupling in solid-state NMR, *Chem. Phys. Lett.*, 426, 459–463, 2006.
- [9] M. Pons *et al.*, Steady-state DQF-COSY spectra using a variable relaxation delay, *J. Magn. Reson.*, 78, 314–320, 1988.
- [10] S. G. J. van Meerten *et al.*, ssNake: A cross-platform open-source NMR data processing and fitting application, *J. Magn. Reson.*, 301, 56–66, 2019.
- [11] B. G. Kim *et al.*, Polysiloxanes containing alkyl side groups: synthesis and mesomorphic behavior, *Macromol. Res.*, 16, 36–44, 2008.
- [12] K. L. Walther *et al.*, $\text{TiO}_2/\text{SiO}_2$ mixed oxide catalysts prepared by sol—gel techniques. Characterization by solid state CP/MAS spectroscopy, *J. Non-Cryst. Solids*, 134, 47–57, 1991.
- [13] M. L. Balmer *et al.*, Solid-State ^{29}Si MAS NMR Study of Titanosilicates, *J. Phys. Chem. B*, 101, 9170–9179, 1997.
- [14] D. P. Burumet *et al.*, Net polarization transfer via a *J*-ordered state for signal enhancement of low-sensitivity nuclei, *J. Magn. Reson.*, 39, 163–168, 1980.
- [15] D. Besghini *et al.*, Time-Domain NMR Elucidates Fibril Formation in Methylcellulose Hydrogels, *Macromolecules*, 56, 4694–4704, 2023.
- [16] P. Klonos *et al.*, Comparative studies on effects of silica and titania nanoparticles on crystallization and complex segmental dynamics in poly(dimethylsiloxane), *Polymer*, 51, 5490–5499, 2010.